Investigation of the removal of Ni(II) from aqueous solution using pomelo fruit peel

Van Phuc Dinh*

Duy Tan University

Abstract:

Pomelo fruit peel, an organic waste, was utilised as a biosorbent to remove Ni(II) from aqueous solutions. Some major factors influencing Ni(II) uptake such as pH, adsorption time, and initial Ni(II) concentration were examined. Several isotherm and kinetic models including the Langmuir, Freundlich, Sips, pseudo-first-order, pseudo-second-order, and intra-diffusion models were fit to the experimental data. Results showed that the Ni(II) uptake obtained an equilibrium at pH=6 after 80 min at 303 K. The Sips isotherm model described the Ni(II) adsorption better than other models and the monoadsorption capacity calculated from the Langmuir model was 9.67 mg/g. The adsorption of Ni(II) followed pseudo-second-order kinetic models with three stages.

Keywords: **biosorption, isotherm models, Ni(II), pomelo fruit peel.**

Classification number: **2.2**

Introduction

In recent years, the expansion of many industries has promote a huge increase in the economy of a large number of developing countries. However, the governments in these countries are faced with significant environmental problems especially those related to heavy toxic metal pollution in the effluent of industrial zones. Ni(II) is one such heavy toxic metal, which has existed in the wastewater of many factories such as electroplating, mineral processing, batteries manufacturing, and so on [1, 2]. As claimed by the World Health Organization (WHO), the limit of Ni(II) concentration in water is 0.005 kg/m³ [2]. Hence, various physicochemical methods have been applied to eliminate Ni(II) from aqueous solutions including adsorption [1-4], precipitation [5, 6], ion-exchange [7, 8] and so on. Among them, adsorption is a promising method since it is simple, low-cost, and easily reused [9, 10].

The use of agricultural waste as biosorbents has attracted many scientists because they are abundantly available, environmentally friendly, and low cost. There are many biosorbents used to remove Ni(II) from aqueous solutions including *Sophora japonica* pod powder [11], *Sargassum* sp. [12], activated banana peel [13], modified plantain peel [14], and Citrus reticulata (fruit peel of orange) [15]. However, the utilisation of pomelo fruit peel (Citrus grandis) as a biosorbent to remove Ni(II) from aqueous solutions has been limited. In previous reports, the pomelo fruit peel was used to adsorb methylene blue [16], Cr(III) [16], Pb(II) [17], and Cd(II) [17]. The obtained results indicated that the pomelo fruit peel is a potential biosorbent to uptake heavy toxic metals and organic molecules from aqueous solutions. Therefore, in this work, the study is extended to Ni(II) adsorption onto the pomelo fruit peel. The $pH_{solution}$, adsorption time, and initial Ni(II) concentration, all of which affect the Ni(II) adsorption, are examined. Some common isotherm and kinetic models are fit to the experimental data to understand the nature of the uptake.

Materials and methods

Preparation of biosorbent

The biosorbent was prepared identical to the author's previous studies [17]. Herein, the pomelo fruit peel was washed by deionised water several times after collection from the Vinh Cuu district, Dong Nai province, Vietnam. The material was then dried in an oven at 80°C within 24 h, prior to cutting into small pieces about 0.5-1 mm in size. Finally, the biosorbent was stored in the oven.

*Email: dinhvanphuc@duytan.edu.vn

Chemicals

The Ni (II) ion was used as an adsorbate, which was prepared by dissolving a Ni(II) standard (1000 mg/l) in deionised (DI) water. The pH adjustment of the investigated solution was carried by using HNO_3 and NaOH with different concentrations. All experimental chemicals used in this work were from Merck (Germany) and were in the analytical reagent grade.

Instruments

The pH meter (Martini instruments, Mi-15, Romania), with buffer solution values of 4.01±0.01, 7.01±0.01, and 10.01±0.01, was used to determine the $pH_{solution}$ values. The material's morphology was examined by ultrahigh resolution SEM (S-4800), whereas the bonding in the materials' structure was found out by Fourier-transform infrared (FT-IR) spectroscopy that was conducted on a Tensor 27 (Bruker, Germany).

In order to determine the Ni(II) concentration before and after the uptake, an atomic absorption spectrophotometer (Shimadzu AA-7000, Japan) was used.

Batch adsorption study

The Ni(II) batch adsorption onto the pomelo fruit peel was carried on IKA magnetic stirrers with a RT 10 P heater. Herein, 0.1 g of the synthesised material was placed into 100 ml flasks together with 50 ml of Ni(II) aqueous solution. These flasks were stirred at a constant rate of 150 rpm. The factors affecting the uptake including pH (2-6), adsorption time (10-240 min), and Ni(II) initial concentration (5-50 mg/l) were examined.

The percentage of the Ni(II) uptake (% removal) and adsorption capacity, Q_e, (mg/g) were determined based on the following equations:

$$\% \text{ Removal} = \frac{(C_o - C_e)}{C_o}.100\% \quad (1)$$

$$Q_e = \frac{(C_o - C_e).V}{m} \quad (2)$$

where the Ni(II) concentration in the aqueous solution before and after the adsorption are symbolised C_o (mg/l) and C_e (mg/l), respectively, V is the volume (l) of metal solution, and m is the mass (g) of the material used.

Adsorption isotherm and kinetic models

In this report, some common adsorption isotherm and kinetic models are fit to the experimental data [17, 18]. These models are given in Table 1.

Table 1. Some common nonlinear isotherm and kinetic models.

Models	Nonlinear forms	Nomenclature
Isotherm models		
Langmuir	$Q_e = \dfrac{Q_m.K_L.C_e}{1+K_L.C_e}$	Q_e (mg/g): amount of adsorbate in the adsorbent at equilibrium.
Freundlich	$Q_e = K_F.C_e^{1/n}$	Q_m (mg/g): maximum monolayer adsorption capacity. K_L (l/mg): Langmuir isotherm constant. K_F [(mg/g).(l/mg)$^{1/n}$]: Freundlich isotherm constant.
Sips	$Q_e = \dfrac{Q_s.C_e^{\beta_s}}{1+\alpha_s.C_e^{\beta_s}}$	n: heterogeneity factor. Q_s (l/g): Sips isotherm model constant. α_s (l/mg): Sips isotherm model constant. β_s: Sips isotherm model exponent.
Kinetic models		
Pseudo-first-order	$Q_t = Q_e\left(1-e^{-k_1 t}\right)$	Q_t (mg/g): adsorption capacity at time t. Q_e (mg/g): adsorption capacity at the equilibrium.
Pseudo-second-order	$Q_t = \dfrac{Q_e^2.k_2.t}{1+k_2.Q_e.t}$	k_1 (min^{-1}): pseudo-first-order model constant. k_2 (g.mg^{-1}.min^{-1}): pseudo-second-order model constant.
Intra-diffusion	$Q_t = k_d t^{1/2} + C$	k_d: intra-diffusion models constant.

Results and discussion

Characterisations of the biosorbent

SEM - EDX analyses: Figs. 1A and 1B show SEM images of pomelo fruit peel at 1.00k and 10.0k magnifications. As seen in these images, the adsorbent surface is very rough, porous, and heterogeneous. These properties are favourable for the heavy metal ion adsorption. The elemental composition of this material was determined by energy-dispersive X-ray spectroscopy (EDX), which is presented in Fig. 1C. The results confirm that the weight percentages of carbon and oxygen were 47.41 and 52.59%, respectively.

Point of zero charge (pH_{PZC}): pH_{PZC} is the pH value of the solution when the material's surface charge is neutral. Indeed, if $pH_{solution}$ is less than pH_{PZC}, the material surface is positively charged. In contrast, the material's surface charge is negative when $pH_{solution} > pH_{PZC}$. Fig. 1D presents the pH_{PZC} of the pomelo fruit peel in this study, which was determined to be 4.6.

FT-IR spectrum: Fig. 2 depicts the vibrations of characteristic groups in the pomelo fruit peel. As seen in this figure, the vibrations of the O-H groups of pectin, cellulose, and lignin are recorded at 3246 cm^{-1}, while the vibrations of the C-H bonds in the CH_2 and CH_3 groups are assigned to wavenumbers 2924 cm^{-1} and 2851 cm^{-1}, respectively. The wavenumbers 1747 cm^{-1} and 1643 cm^{-1} are related to the C=O groups [19]. Finally, the wavenumbers 1107 cm^{-1} and 1026 cm^{-1} confirm the C-O group's stretching vibrations in the lignin structure of pomelo fruit peel [16].
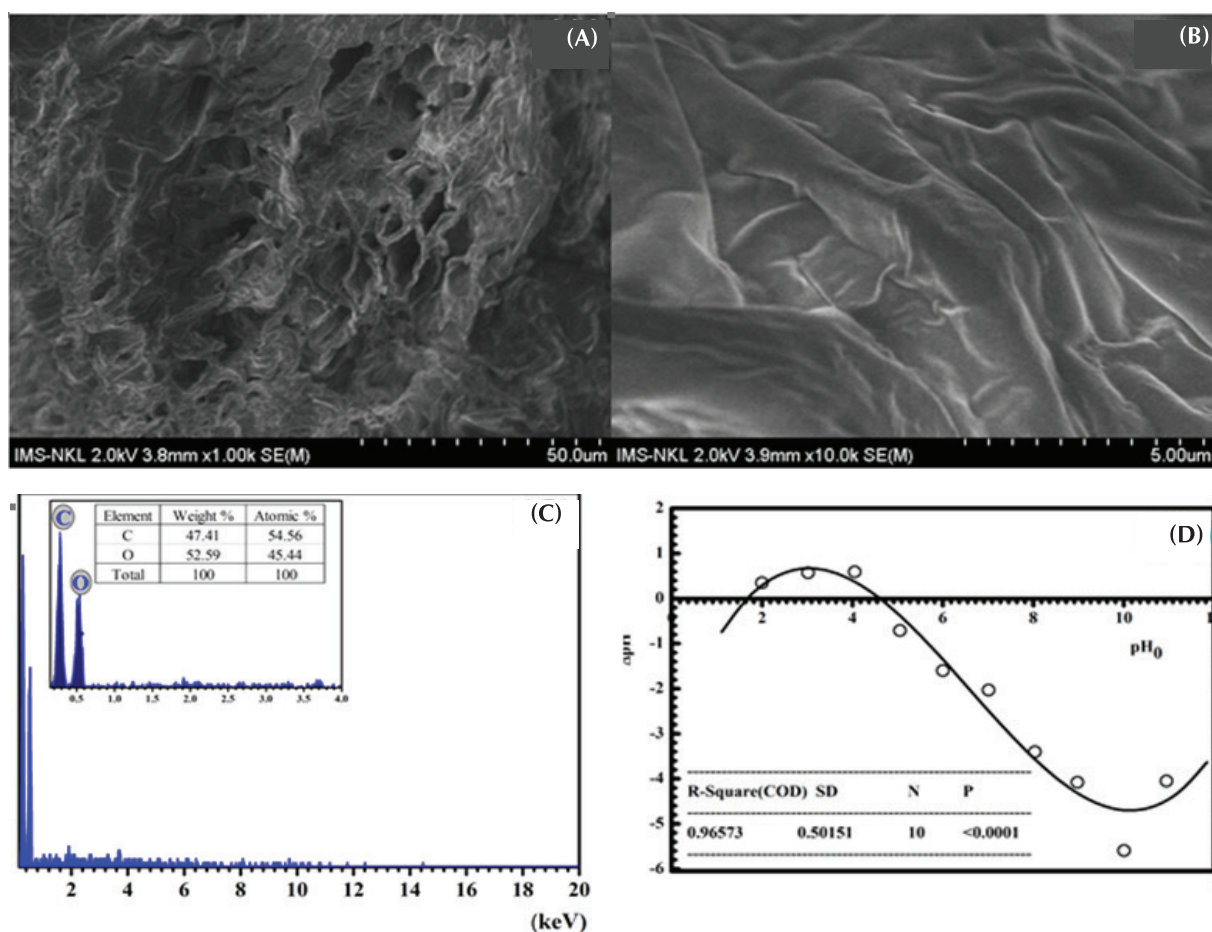
Fig. 1. (A, B) SEM images at different magnifications, (C) the EDX spectrum, and (D) pH$_{PZC}$ of the pomelo fruit peel.
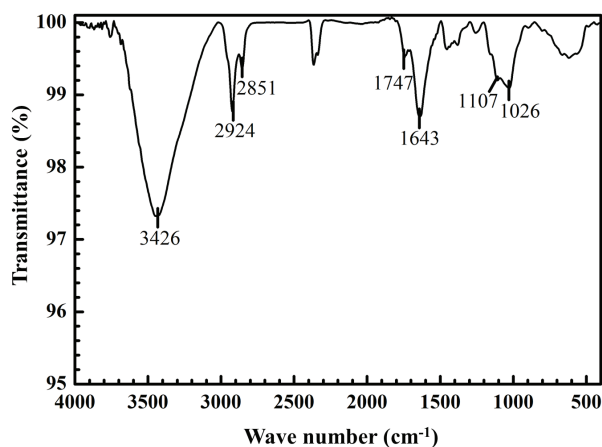

Fig. 2. FT-IR spectrum of pomelo fruit peel.

Factors affecting the removal of Ni(II)

pH$_{solution}$: pH$_{solution}$ directly affects the removal of Ni(II) due to its effects on the formation of different complexes of Ni(II) and the surface charge of materials. Fig. 3A indicates

that the uptake of Ni(II) rises rapidly when pH$_{solution}$ is increased from 2 to 4. In the next stage, there is a slight increase in the adsorption prior to obtaining the maximum at pH=6. The increase in pH$_{solution}$ from 2 to 6 leads to a change in material surface charge from positive to negative. At pH$_{solution}$>pH$_{PZC}$=4.6, the material's surface charge is negative, which leads to a rise in Ni(II) adsorption due to the electrostatic attraction between Ni(II) cations and the negatively-charged material surface [20, 21]. However, the author observed that nickel (II) hydroxide can be formed at pH$_{solution}$>6. Therefore, pH=6 is chosen for further experiments.

The adsorption time: the influence of the adsorption time on the Ni(II) biosorption by pomelo fruit peel is indicated in Fig. 3B. The uptake rate of Ni(II) significantly increases prior to reaching equilibrium at 80 min and then remained stable. Therefore, the optimal adsorption time was determined to be 80 min.
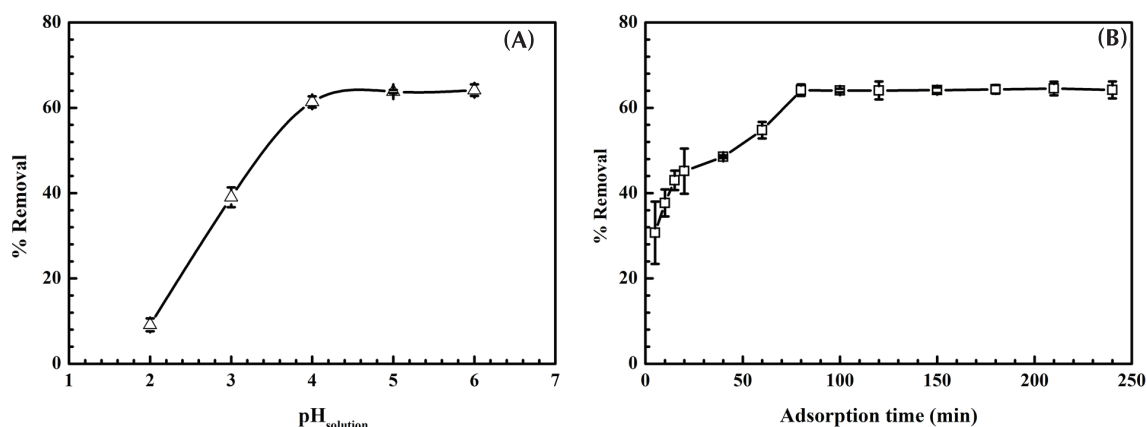
Fig. 3. Plots of the effects of (A) pH$_{solution}$ and (B) adsorption time on Ni(II) adsorption.
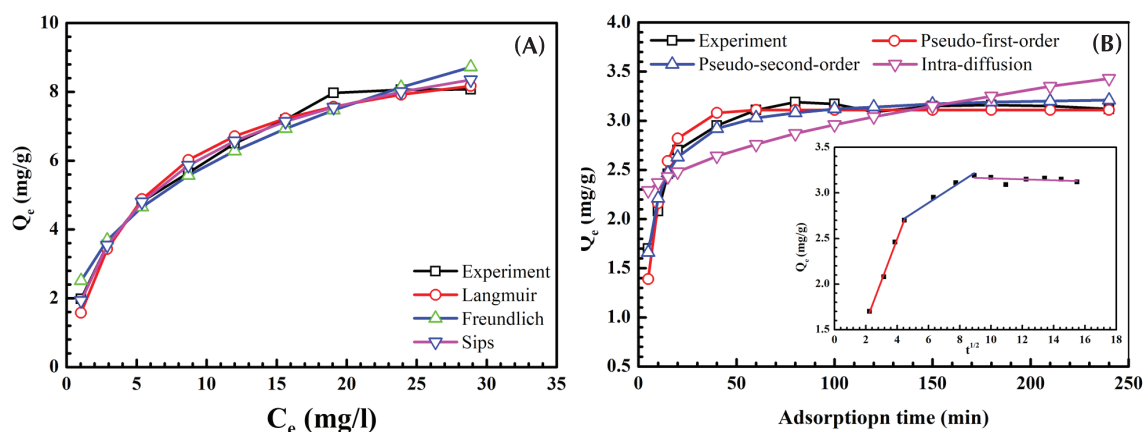

Fig. 4. Plots of (A) isotherm models and (B) kinetic models of the Ni(II) adsorption onto pomelo fruit peel.

Isotherm studies

The plots of several common isotherm models including Langmuir, Freundlich, and the Sips models are presented in Fig. 4A. The nonlinear isotherm parameters of these models are listed in Table 2. According to calculated RMSE and χ^2 values, the experimental data had a better fit with the Sips model than the others as determined by the smallest RMSE and χ^2 values. The main reason is that the Langmuir and Freundlich models are constrained by the adsorbates' concentration, while the Sips model combines these models and overcomes this problem [18]. Furthermore, the Langmuir maximum monolayer adsorption capacity was 9.67 mg/g, which is higher than other biosorbents such as hazelnut shell, fly ash, rice husk, banana peel, and doum palm (Hyphaene thebaica L.) (Table 3). The n value (n=2.67) evaluated from the Freundlich model ranges from 1 to 10 and indicates how favourable conditions are for adsorption [18, 22]. However, the Ni(II) adsorption capacity is lower than Pb(II), Cd(II), and Cr(III) when the same pomelo fruit peel is used [16, 17]. This shows that the pomelo fruit peel is a potential material for removing heavy metals from aqueous solutions.

Table 2. Parameters of nonlinear isotherm models at temperature of 303 K.

Isotherm models	Parameters	
Langmuir	K_L (l/mg)	0.1891
	Q_m (mg/g)	9.67
	RMSE	0.2625
	R^2	0.9854
	χ^2	0.1413
Freundlich	n	2.67
	K_F [(mg/g).(l/mg)$^{1/n}$]	2.48
	RMSE	0.3752
	R^2	0.9701
	χ^2	0.2519
Sips	Q_s (l/g)	2.25
	α_s (l/mg)	0.1938
	β_s	0.7667
	RMSE	0.1975
	R^2	0.9917
	χ^2	0.0428

Table 3. Maximum adsorption capacities of several biosorbents for the Ni(II) uptake from aqueous solutions [23-27].

Biosorbents	Adsorptive condition	Adsorption capacity (mg/g)	References
Doum palm (Hyphaene thebaica L.)	pH=7.00, t=120 min	3.24	[1]
Banana peel	pH=6.89, t=24 h	6.88	[23]
Rice husk	pH=6.00, t=120 min	8.86	[24]
Fly ash	pH=8.00, t=60 min	0.03	[25]
Hazelnut shell	pH=7.00, t=180 min	7.18	[26]
Cone biomass of Thuja orientalis	pH=4.00, t=7 min	12.42	[27]
Brown algae *Sargassum* sp.	pH=6.00, t=90 min	50.97	[12]
Pomelo fruit peel	pH=6.00, t=80 min	9.67	This study

Kinetic studies

Figure 4B and Table 4 present the plots of the kinetic models and non-linear parameters, respectively. Clearly, the pseudo-second-model fit to the experimental data is better than the pseudo-first-order model owing to the small RMSE and χ^2 values. However, both models cannot describe the mass transfer of cations onto the material's surface. The

Table 4. Parameters of nonlinear kinetic models at 303 K.

Kinetic models	Parameters	
	C_o (mg/l)	10
	$Q_{e\,(exp)}$ (mg/g)	3.2
Pseudo-first-order model	$Q_{e\,(cal)}$ (mg/g)	3.11
	k_1 (min^{-1})	0.1190
	RMSE	0.1185
	R^2	0.9395
	χ^2	0.0831
Pseudo-second-order model	$Q_{e\,(cal)}$ (mg/g)	3.27
	k_2 (g.mg^{-1}.min^{-1})	0.0633
	RMSE	0.0678
	R^2	0.9802
	χ^2	0.0208
Intra-diffusion model	k_d	0.0865
	C	2.0945
	RMSE	0.2858
	R^2	0.6480
	χ^2	0.4217

intra-diffusion model is therefore applied to determine the Ni(II) adsorption kinetic onto pomelo fruit peel. As seen from the plot of Q_e versus $t^{1/2}$ in Fig. 4B, the removal of Ni(II) includes three stages. Firstly, Ni(II) cations are steeply transferred from the solution to the material's surface within about 20 min. In the next stage, the Ni(II) uptake more gradually occurs from 20 to 80 min, prior to obtaining the equilibrium in the last stage. From the nonzero C value calculated from the intra-diffusion model, the Ni(II) uptake follows not only the intra-diffusion process but also two or more different mechanisms [28, 29].

Conclusions

The Ni(II) adsorption onto pomelo fruit peel was investigated. The results showed that the Ni(II) uptake reached equilibrium at pH=6.00 after 80 min at 303 K. Kinetic studies showed that the Ni(II) uptake was controlled by various mechanisms. The Langmuir maximum adsorption capacity was 9.67 mg/g, which was higher than some other biosorbents. Therefore, pomelo fruit peel can be used as a promising, eco-friendly, and low-cost material to eliminate Ni(II) from the effluent.

COMPETING INTERESTS

The author declares that there is no conflict of interest regarding the publication of this article.

REFERENCES

[1] M. El-Sadaawy, O. Abdelwahab (2014), "Adsorptive removal of nickel from aqueous solutions by activated carbons from doum seed (*Hyphaenethebaica*) coat", *Alexandria Engineering Journal*, **53(2)**, pp.399-408.

[2] H. Pahlavanzadeh, M. Motamedi (2020), "Adsorption of nickel, Ni(II), in aqueous solution by modified zeolite as a cation-exchange adsorbent", *Journal of Chemical and Engineering Data*, **65(1)**, pp.185-197.

[3] S. Ghrab, et al. (2018), "Adsorption of nickel(II) and chromium(III) from aqueous phases on raw smectite: kinetic and thermodynamic studies", *Arabian Journal of Geosciences*, **11**, DOI: 10.1007/s12517-018-3749-2.

[4] K. Kadirvelu, K. Thamaraiselvi, C. Namasivayam (2001), "Adsorption of nickel(II) from aqueous solution onto activated carbon prepared from coirpith", *Separation and Purification Technology*, **24(3)**, pp.497-505.

[5] S. Janyasuthiwong, et al. (2015), "Effect of pH on Cu, Ni and Zn removal by biogenic sulfide precipitation in an inversed fluidized

bed bioreactor", *Hydrometallurgy*, **158**, pp.94-100.

[6] J. Esalah, M.M. Husein (2008), "Removal of heavy metals from aqueous solutions by precipitation-filtration using novel organo-phosphorus ligands", *Separation Science and Technology*, **43(13)**, pp.3461-3475.

[7] N.H. Shaidan, U. Eldemerdash, S. Awad (2012), "Removal of Ni(II) ions from aqueous solutions using fixed-bed ion exchange column technique", *Journal of the Taiwan Institute of Chemical Engineers*, **43(1)**, pp.40-45.

[8] N.K. Amin, O. Abdelwahab, E.S.Z. El-Ashtoukhy (2015), "Removal of Cu(II) and Ni(II) by ion exchange resin in packed rotating cylinder", *Desalination and Water Treatment*, **55(1)**, pp.199-209.

[9] V.-P. Dinh, et al. (2020a), "Chitosan-MnO₂ nanocomposite for effective removal of Cr(VI) from aqueous solution", *Chemosphere*, **257**, DOI: 10.1016/j.chemosphere.2020.127147.

[10] E.N. Zare, M.M. Lakouraj, A. Ramezani (2015), "Effective adsorption of heavy metal cations by superparamagnetic poly (aniline-co-m-phenylenediamine)@ Fe₃O₄ nanocomposite", *Advances in Polymer Technology*, **34(3)**, DOI: 10.1002/adv.21501.

[11] M.W. Amer, R.A. Ahmad, A.M. Awwad (2015), "Biosorption of Cu(II), Ni(II), Zn(II) and Pb(II) ions from aqueous solution by Sophora japonica pods powder", *International Journal of Industrial Chemistry*, **6(1)**, pp.67-75.

[12] C.E.R. Barquilha, et al. (2019), "Biosorption of nickel(II) and copper(II) ions by *Sargassum* sp. in nature and alginate extraction products", *Bioresource Technology Reports*, **5**, pp.43-50.

[13] Z. Liu, et al. (2014), "Performance study of heavy metal ion adsorption onto microwave-activated banana peel", *Desalination and Water Treatment*, **52(37-39)**, pp.7117-7124.

[14] Z.N. Garba, N.I. Ugbaga, A.K. Abdullahi (2016), "Evaluation of optimum adsorption conditions for Ni(II) and Cd(II) removal from aqueous solution by modified plantain peels (MPP)", *Beni-Suef University Journal of Basic and Applied Sciences*, **5(2)**, pp.170-179.

[15] M. Ajmal, et al. (2000), "Adsorption studies on Citrus reticulata (fruit peel of orange): removal and recovery of Ni(II) from electroplating wastewater", *Journal of Hazardous Materials*, **79(1)**, pp.117-131.

[16] V.-P. Dinh, et al. (2019), "Insight into the adsorption mechanisms of methylene blue and chromium(III) from aqueous solution onto pomelo fruit peel", *RSC Advances*, **9(44)**, pp.25847-25860.

[17] V.-P. Dinh, et al. (2020b), "Primary biosorption mechanism of lead (II) and cadmium (II) cations from aqueous solution by pomelo (*Citrus maxima*) fruit peels", *Environmental Science and Pollution Research*, DOI: 10.1007/s11356-020-10176-6.

[18] K.Y. Foo, B.H. Hameed (2010), "Insights into the modeling of adsorption isotherm systems", *Chemical Engineering Journal*, **156(1)**, pp.2-10.

[19] M. Torab-Mostaedi, et al. (2013), "Equilibrium, kinetic, and thermodynamic studies for biosorption of cadmium and nickel on grapefruit peel", *Journal of the Taiwan Institute of Chemical Engineers*, **44(2)**, pp.295-302.

[20] A.M. Cardenas-Peña, J.G. Ibanez, and R. Vasquez-Medrano (2012), "Determination of the point of zero charge for electrocoagulation precipitates from an iron anode", *Int. J. Electrochem. Sci.*, **7(7)**, pp.6142-6153.

[21] M. Singh, et al. (2010), "Synthesis, characterization and study of arsenate adsorption from aqueous solution by α-and δ-phase manganese dioxide nanoadsorbents", *Journal of Solid State Chemistry*, **183(12)**, pp.2979-2986.

[22] H. Liu, F. Zhang, Z. Peng (2019), "Adsorption mechanism of Cr(VI) onto GO/PAMAMs composites", *Scientific Reports*, **9(1)**, DOI: 10.1038/s41598-019-40344-9.

[23] G. Annadurai, R.S. Juang, D.J. Lee (2003), "Adsorption of heavy metals from water using banana and orange peels", *Water Science and Technology*, **47(1)**, pp.185-190.

[24] M. Bansal, et al. (2009), "Use of agricultural waste for the removal of nickel ions from aqueous solutions: equilibrium and kinetics studies", *International Journal of Civil and Environmental Engineering*, **3(3)**, pp.174-180.

[25] M. Rao, A.V. Parwate, A.G. Bhole (2002), "Removal of Cr⁶⁺ and Ni²⁺ from aqueous solution using bagasse and fly ash", *Waste Management*, **22(7)**, pp.821-830.

[26] E. Demirbaş, et al. (2002), "Removal of Ni(II) from aqueous solution by adsorption onto hazelnut shell activated carbon: equilibrium studies", *Bioresource Technology*, **84(3)**, pp.291-293.

[27] E. Malkoc (2006), "Ni(II) removal from aqueous solutions using cone biomass of Thuja orientalis", *Journal of Hazardous Materials*, **137(2)**, pp.899-908.

[28] S. Vasiliu, et al. (2011), "Adsorption of cefotaxime sodium salt on polymer coated ion exchange resin microparticles: kinetics, equilibrium and thermodynamic studies", *Carbohyd. Polym.*, **85(2)**, pp.376-387.

[29] V.-P. Dinh, et al. (2018), "Insight into adsorption mechanism of lead(II) from aqueous solution by chitosan loaded MnO₂ nanoparticles", *Materials Chemistry and Physics*, **207**, pp.294-302.